Talanta 106 (2013) 360–366

Contents lists available at SciVerse ScienceDirect

Talanta

journal homepage: www.elsevier.com/locate/talanta

A novel electrochemical immunosensor based on magnetosomes for detection of staphylococcal enterotoxin B in milk

Longyun Wu [a], Bo Gao [a], Fang Zhang [a], Xiulan Sun [a,*], Yinzhi Zhang [a], Zaijun Li [a,b]

[a] State Key Laboratory of Food Science and Technology, School of Food Science of Jiangnan University, Wuxi, Jiangsu 214122, China
[b] School of Chemical and Material Engineering of Jiangnan University, Wuxi, Jiangsu 214122, China

ARTICLE INFO

Article history:
Received 13 September 2012
Received in revised form
28 December 2012
Accepted 30 December 2012
Available online 16 January 2013

Keywords:
Polyaniline nano-gold composite
Magnetosomes
Electrochemical immunosensor
Staphylococcal enterotoxin B

ABSTRACT

In this paper, a novel electrochemical immunosensor to detect staphylococcal enterotoxin B based on bio-magnetosomes, polyaniline nano-gold composite and 1,2-dimethyl-3-butylimidazolium hexafluorophosphate ionic liquid, was developed, and found to exhibit high sensitivity and stability. The specific antibody to staphylococcal enterotoxin B conjugated with the magnetosomes showed rapid immunoreactions and good dispersion, which contributed to the formation of a nanostructurally smooth and dense film on the surface of a gold electrode. Polyaniline nano-gold composite and 1,2-dimethyl-3-butylimidazolium hexafluorophosphate ionic liquid were used to modify the electrode as mediators to improve the electron transfer and offer an excellent biocompatible microenvironment for the antibody to retain its activity to enhance the response of the electrochemical sensor. Under optimal conditions, the developed immunosensor showed a good linear response in the range from 0.05 to 5 ng/mL (R^2=0.9957) with a detection limit as low as 0.017 ng/mL, compared with the one without magnetosomes (0.05–5 ng/mL, 0.033 ng/mL), this developed immunosensor showed a wider response range and a reduced detection limit. And a good specificity with little adsorption to staphylococcal enterotoxin A, C and Na^+, K^+, Ca^{2+} was obtained. Moreover, the immunosensor exhibited a good long-time stability at 4 °C reaching up to 60 days, which showed a relatively long working life. Meanwhile the immunosensor could be regenerated four times using NaOH elution. The sensor also displayed a good repeatability with a relative standard deviation of 5.02% for staphylococcal enterotoxin B detection (1 ng/mL, n=9). Furthermore, high recoveries in milk samples from 81% to 118% were achieved and successfully applied to milk sample detection. The obtained results demonstrate that the developed electrochemical immunosensor is a promising tool for the detection of staphylococcal enterotoxin B in food.

1. Introduction

Staphylococcal enterotoxins (SEs) are a group of toxic proteins with similar structure produced by *Staphylococcus aureus* [1,2]. SEs are naturally found in foods that are rich in proteins, such as meat and milk [3,4]. The classical serotypes of SEs are SEA, SEB, SEC, SED and SEE; however, new serotypes have been found recently, including SEG, SEE, SEI, SEJ, SEK, SEL, SEM, SEN, SEO [5]. Among them, SEB was found to be the most potent SEs, with a half-lethal dose of about 20 ng/kg [6]. Aside from being the main toxin responsible for staphylococcal food-borne diseases, SEB has been produced by some countries as a biological weapon owing to its high morbidity rate, inherent stability and ease of dissemination [1,6]. Therefore, a cost-effective, rapid and sensitive analytical method is required for the determination of SEB in food at low concentration levels.

During the past few decades, a wide range of methods has been employed to detect SEB, ranging from the previous gel diffusion test to various rapid methods [7], resulting in an improved detection limit and sensitivity. Enzyme-linked immunosorbent assays (ELISA), liquid-chromatography–mass spectrometry (LC–MS) and real-time fluorescence polymerase chain reaction (RT-PCR) were commonly used methods for SEB detection at nanogram and pictogram level, and the detection limits of SEB were 0.1 ng/mL [8], 3 pmol/mL [9] and 250 colony-forming units [10], respectively. However, all of these three methods had shortcomings, ELISA prone to false positive

Abbreviations: SEs, staphylococcal enterotoxins; SEB, staphylococcal enterotoxin B; SEA, staphylococcal enterotoxin A; SEC, staphylococcal enterotoxin C; (PANI)/Au, polyaniline nano-gold composite; RSD, relative standard deviation; EDC · HCL, 1-[3-(dimethylamino)propyl]-3-ethylcarbodiimide hydrochloride; [D(n-C4)Im][PF6], 1,2-dimethyl-3-butylimidazolium hexafluorophosphate; BSA, bovine serum albumin; PBS, phosphate buffer solution; CD, circular dichroism; CV, cyclic voltammetry; EIS, electrochemical impedance spectroscopy

* Corresponding author. Tel.: +86 510 85329015; fax: +86 51085328726.
E-mail address: sxlzzz@jiangnan.edu.cn (X. Sun).

0039-9140/$ - see front matter © 2013 Elsevier B.V. All rights reserved.
http://dx.doi.org/10.1016/j.talanta.2012.12.053

due to the influence of food matrix, the LC–MS are time-consuming as well as large specialized equipment was required, the RT-PCR need special operation skills and expensive [11]; all of these limit their application in the detection of SEB in the field.

Over the last few years, several antigen/antibody based biosensor for the detection of SEB [12–18] has been developed. Electrochemical immunosensors with the merits of rapid detection, low cost, and high sensitivity have attracted much interest and have been widely applied to the detection of SEB [13,19]. Such immunosensors are mainly dependent on changes of impedance after incubation with SEB. Furthermore, a series of improvements have been carried out to enhance the sensitivity and reduce the detection limit of the electrochemical immunosensors [20–24], which are crucial for achieving low detection limits.

Recently, magnetic nanoparticles have increasingly been applied to the electrochemical immunosensors [25–27], because of their superior features, such as easy purification and easy concentration from crude samples owing to their superparamagnetic properties, thereby eliminating the influence of the food matrix [28–30]. Additionally, magnetic nanoparticles have a large surface area to immobilize biomolecules, which provides a low detection limit [23,31,32]. Furthermore, biosensors that rely on the use of magnetic nanoparticles as mediators enable the immunological reaction to be conducted quickly on the electrode surface [33,34], which has the effect of reducing the time required for detection. However, the aggregation of magnetic nanoparticles is widely known to limit their utilization in sensors [35,36]. To overcome this shortcoming, novel magnetosomes were produced by magnetotactic bacteria purchased from the American Type Culture Collection (ATCC700264). These magnetosomes are regarded as promising magnetic nanoparticles and widely researched owing to their good dispersity, biocompatibility and easy conjugation of biomolecules [37–41].

Herein, we firstly present a novel electrochemical immunosensor based on magnetosomes to detect SEB, the fabrication process was explained in Scheme 1. Briefly, the gold electrode was immersed in an aqueous solution of polyaniline nano-gold composite (PANI/Au) solution, and the solution was kept overnight at room temperature until the gold electrode was completely modified. PANI/Au is considered as an excellent nanoscale electrically conductive polymer and used as an electronic transmission device to amplify signals [42,43]. Then, 5 mL 1,2-dimethyl-3-butylimidazolium hexafluorophosphate ([D(n-C4)Im][PF6]) ionic liquid was deposited onto the modified surface of the gold electrode and left to stand for 60 min at room temperature. The [D(n-C4)Im][PF6] ionic liquid was used as a potential electrolyte owing to its intrinsic conductivity and wide electrochemical window [44–46]. Then, 10 μL SEB immuno-magnetosomes (40 μg/mL) was deposited onto the surface of the gold electrode and incubated at 37 °C for 80 min. Finally, the gold electrode surface was blocked for 100 min. We investigated the performance of the magnetosomes-based immunosensor, including its electrochemical behavior in $Fe(CN)_6^{3-/4-}$ solution, the limit of detection, specificity, recovery test, reproducibility and stability, meanwhile the magnetosomes-based immunosensor was successfully applied to detect SEB in milk products.

2. Experimental

2.1. Apparatus and electrodes

Cyclic voltammogram (CV) and electrochemical impedance spectroscopy (EIS) were performed in a CHI760C electrochemical workstation (Shanghai Chenhua Instruments, Shanghai, China) equipped with a conventional three-electrode system, and all measurements were carried out at room temperature in $Fe(CN)_6^{3-/4-}$ working solution. In this three electrodes configuration, a modified gold electrode was used as a working electrode, a saturated calomel electrode as a reference electrode, and a platinum wire as a counter electrode. Before the modification of gold electrode, the gold electrode was first dipped into a freshly prepared solution of 3:7 (v/v) 30% H_2O_2 and 98% H_2SO_4 for 20 min, followed by rinsing with ultrapure water. The cleaned gold electrode was subsequently polished with 0.3 μm and 0.05 μm alumina slurries, successively, and then washed again with ultrapure water. Then, the gold electrode was immersed sequentially in ethanol and ultrapure water in an ultrasonic bath for 5 min. Finally, the CV of the cleaned gold electrode was scanned until a mirror-shine surface was obtained. Prior to each experiment, the buffer solutions were purged with highly purified nitrogen for at least 30 min and a nitrogen atmosphere environment was maintained in the electrochemical measurements. Scanning electron microscope (SEM) (JEOL JSM-6390LA, Electronic Incorporated Company, Japan) was used to characterize magnetosomes and the surface of the modified gold electrode, the detail detection conditions were as follows: the accelerating voltage was 0.5–30 kV with a 1 pA–1 μA SEM electron beam. Transmission electron microscopy (TEM) (JEOL JEM-2100 (HR), Electronic Incorporated Company, Japan), Fourier transform infrared spectrometer (FT-IR) (NICOLET MEXUS 470, Thermo Electron Corporation, Japan), Circular dichroism-stopped-flow spectrophotometer (CD) (Mos-450 AF, Bio-logic Company, France) and Plate reader (Multiskan MK3, Thermo Lab Systems Company, Shanghai) were used to characterize the prepared materials. The TEM images were performed at a 200 kV accelerating voltage with a magnification factor of 50–6000. FT-IR detection conditions were as follows: resolution, 0.5–16 cm^{-1}; test range of wave numbers, 4000–400 cm^{-1}; and wave number precision, < 0.01 cm^{-1}. The CD spectra were carried out in the far-UV region from 190 nm to 250 nm under a nitrogen atmosphere at room temperature using a cell with a 1 mm path length at a sample concentration of 1 mg/mL, and each spectrum obtained was the average of at least three runs with a bandwidth of 1.0 nm at an accuracy of 0.1 nm. The microplate reader was used to measure the

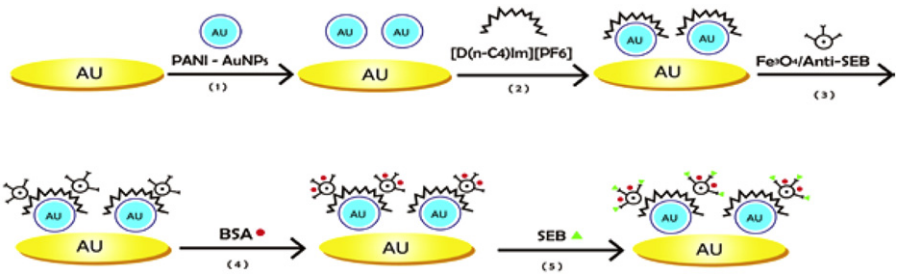

Scheme 1. Fabrication process of the immunsensor: (1) self-assembled PANI/Au; (2) self-assembled $[D(n\text{-}C_4)Im][PF_6]$; (3) SEB immuno-magnetosomes; (4) blocking with BSA; and (5) detection of SEB.

absorbance of the immuno-magnetosomes sample at a 450 nm wavelength.

2.2. Reagents and materials

Hydrogen tetrachloraurate (III) trihydrate ($HAuCl_4$, 99%) and 1-[3-(dimethylamino)propyl]-3-ethylcarbodiimide hydrochloride (EDC·HCL) were purchased from Sigma-Aldrich (Shanghai, China). SEB ELISA kit was purchased from Xiang-Feng Biotech (ShangHai) company (Shanghai, China).The phosphate buffer solution (PBS) consisted of 0.2 g KH_2PO_4, 2.9 g $Na_2HPO_4 \cdot H_2O$, 8 g NaCl and 0.2 g KCl (pH=7.4). Biological magnetosomes prepared from Magnetotactic bacterium AMB-1 strains which were purchased from the American Type Culture Collection (ATCC700264) [47]. They were made in a modified magnetic spirillum growth medium (MSGM) [48,49]. Polyclonal anti-SEB antibodies, PANI/Au were prepared in our lab according to the reported procedure [50–53]. [D(n-C_4)Im][PF_6] was prepared according to the reported procedure [54]. Ultrapure water was used for cleaning the electrodes after each step. Unless otherwise specified, all chemicals were of analytical grade. Furthermore, to accurately calculate the coupling ratio, a BCA Protein Assay Kit (containing SK3061-1 reagents A, SK3061-2 reagents B, SK3061-3 reagents C and SK3061 bovine serum albumin (BSA) standards solution) were purchased from the Sangon Biotech (Shanghai) Company (Shanghai, China). The measurement was carried out as follows: the BCA working reagent was prepared by mixing 1.5 mL of reagent A, 1.44 mL of reagent B and 60 μL of reagent C in a 4 mL centrifugal tube. BSA standard solution (40 μg/mL) was prepared by mixing 40 μL of BSA standard solution and 496 mL of ultrapure water. A standard curve was achieved by measuring at different concentrations (0.0 ng/mL, 0.5 ng/mL, 1 ng/mL, 2 ng/mL, 5 ng/mL, 10 ng/mL, 15 ng/mL, 20 ng/mL, 40 ng/mL) of BSA standard solution at 37 °C for 2 h.

2.3. Methods

2.3.1. Synthesis of [D(n-C4)im][PF6], PANI/Au and preparation of SEB antibody-functionalized magnetosomes

The [D(n-C_4)Im][PF_6] was prepared according to the reported procedure [54] and then stored in a vacuum dryer until use. The [D(n-C_4)Im][PF_6] was characterized by FT-IR with the KBr method.

The PANI/Au was prepared as follows: 125 μL of $HAuCl_4$ solution was added to 50 mL of ultrapure water until boiling. A sodium citrate solution (4%, 400 μL) was added to the mixture, which was then stirred for 10 min. Then, 600 μL of NaOH solution (0.2 mol/L), 500 μL of phenylamine solution (0.1 mol/L) and 750 μL of sodium persulfate solution (0.1 mol/L) were added sequentially to the mixture with continuous stirring, and continually boiled for 40 min. The resultant mixture was cooled to room temperature with distilled water up to 50 mL, and then stored at 4 °C until use. PANI/Au was characterized by FT-IR and TEM.

The SEB antibody-functionalized magnetosomes were synthesized through the method of covalent bonding. First, 1 mL of a magnetosomes solution (1 mg/mL) was added to 2 mL of EDC·HCL solution (1 mg/mL) by magnetic stirring at 4 °C or 12 h. Then, the prepared SEB poly-antibody was added for another 12 h at 4 °C. Afterwards, the SEB antibody-functionalized magnetosomes were separated by centrifugation at 8000 rpm for 20 min. The obtained immuno-magnetosomes were suspended using phosphate buffer solution adjusted to pH 7.4, and then stored at 4 °C until use. The antibody-functionalized magnetosomes were characterized by FT-IR, CD and BCA experiment.

2.3.2. Fabrication of electrochemical sensor based on immuno-magnetosomes

The electrochemical immunosensor was assembled layer-by-layer via direct physical absorption, the fabrication process was explained in Scheme 1. Briefly, the gold electrode was immersed in an aqueous solution of PANI/Au solution, and the solution was kept overnight at room temperature until the gold electrode was completely modified. Then, 5 mL [D(n-C_4)Im][PF_6](5%) was deposited onto the modified surface of the gold electrode and left to stand for 60 min at room temperature. Then, 10 μL SEB immuno-magnetosomes (40 μg/mL) was deposited onto the surface of the gold electrode and incubated at 37 °C for 80 min. Finally, the gold electrode surface was blocked with 10 μL BSA-PBS solution for 100 min. The fabricated sensor could be used for the rapid detection of SEB almost 20 min after incubation.

2.3.3. Electrochemical measurements

10 μL of different concentrations SEB standard solution was dropped onto the surface of above fabricated electrode. After incubation at 37 °C for 25 min, electrochemical measurements were carried out by using a CHI760C electrochemical workstation. CV was performed at a range from −0.2 V to 0.6 V with a scanning speed of 0.1 V/s. EIS was measured in the frequency range of 1–100 Hz in a potential of 0.20 V, a voltage amplitude of 5 mV and a standing time 2 s. All experiments were performed in $Fe(CN)_6^{3-/4-}$ working solution, and the impedance, Z, was expressed in terms of a real (Z') and an imaginary ($-Z''$) component.

2.3.4. Detection of SEB in milk

For the application of as-prepared immunosensor in real samples, milk samples, free of SEs (detected using SEB ELISA kit and found that almost no SEB exist in these milk samples), were spiked with different concentrations (0.5 ng/mL, 2 ng/mL, 4 ng/mL) of SEB. Then, these solutions were isolated by centrifugation at 10,000 rpm for 10 min. The supernatant was diluted in 0.01% w/v in PBS buffer solutions (pH 7.4) and analyzed by the protocol of 2.3.3. The recovery was as follows: recovery=found concentration/theoretical concentration × 100%.

3. Results and discussion

3.1. Characteristics of prepared materials

Fig. S1 depicts the FT-IR spectrum of [D(n-C_4)Im][PF_6] with several typical features. First, the weak and narrow absorption peak centered at around 3672 cm^{-1} is attributed to the stretching vibration of P–F. Two moderate intense and narrow absorption peaks at around 3161 cm^{-1}, 3120 cm^{-1} and 2971 cm^{-1}, 2939 cm^{-1} are attributed to the stretching vibrations of the C–H bands about the imidazole ring and aliphatic compounds, respectively. In the lower frequency range, several intense bands were observed, which are consistent with the characteristic bands of the imidazole ring at around 1573 cm^{-1} and 1464 cm^{-1} and the weak peaks at around 1390 cm^{-1} and 1460 cm^{-1} attributed to the bend vibration of CH_3 and CH_2, respectively. In addition, the band at 1172 cm^{-1} represents the bend vibration of C–H of the imidazole ring, while the bands at 1140 cm^{-1}, 1196 cm^{-1} and 835 cm^{-1} correspond to the stretching vibrations of S=O, C–F and P–F, respectively.

Fig. S2 shows TEM images of PANI/Au (Fig. S2a, c) and Au (Fig. S2b), from which the difference in the morphologies is described. Compared with the Au nanoparticles, PANI/Au exhibited a smooth and transparent film at the surface of the Au corresponding to the formation of a core-shell structure. In addition, the FT-IR spectra

of PANI/Au (Fig. S2d) provide further proof of the formation of the core-shell structure: the sharp absorption peak at around 3420 cm^{-1} indicates the stretching vibration of N–H. The moderately intense and narrow absorption peak at around 1580 cm^{-1} is characteristic of the stretching vibration of C–N associated with the benzene ring, and the bands at 1350 cm^{-1} and 610 cm^{-1} are attributed to the bend vibration of C–H bands. In conclusion, the results confirm the successful linking of PANI to Au.

As shown in Fig. 1, SEM images of the as-prepared magnetosomes (Fig. 1a) and antibody-functionalized magnetosomes (Fig. 1b) showed apparently the difference of their morphologies. Compared with the magnetosomes, the antibody-coated magnetosomes exhibited a larger diameter and a better dispersity. From the FT-IR spectrum (Fig. 1c) we can see, except the typical absorption peak of the N–H and/or O–H stretching vibration bands centered at around 3400 cm^{-1} and the characteristic absorption peak of C=O stretching vibration, N–H bend vibration at around 1650 cm^{-1} and 1520 cm^{-1}, there are several special and significantly enhanced absorption peaks were shown in Fig. 1c between SEB antibody and SEB antibody-functionalized magnetosomes. At first, a relatively intensive band at around 590 cm^{-1} was observed, which is the typical absorption peak of Fe–O stretching vibration, Additionally, three significantly enhanced absorption peaks at around 1073 cm^{-1}, 1162 cm^{-1} and 1400 cm^{-1} were also observed, which are characteristic absorption peak of C–N stretching vibration of the amine. Consequently, all the above bands support the successful coupling of the magnetosomes to SEB antibodies. On the other hand, as shown in Fig. 1d, the blue shift of the negative circular dichroism band of β-sheet associated with the general structure of the antibody from 198 nm to 193 nm also indicate the interaction of the SEB antibodies with Fe_3O_4; finally, the coupling ratio

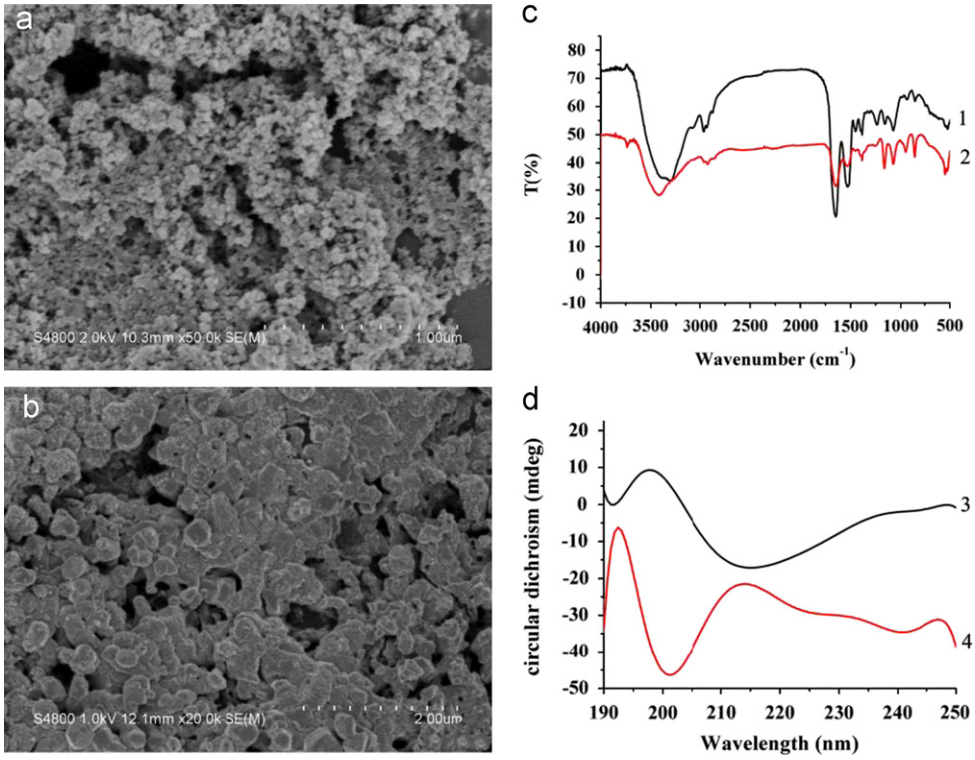

Fig. 1. SEM micrograph and FT-IR spectra of magnetosomes and SEB antibodies functionalized magnetosomes: SEM micrograph of magnetosomes (a); SEM micrograph of immuno-magnetosomes (b); FT-IR spectra of anti-SEB antibodies (1), anti-SEB antibodies functionalized magnetosomes (2); CD spectra of SEB antibody (3) and SEB antibody-functionalized magnetosomes (4).

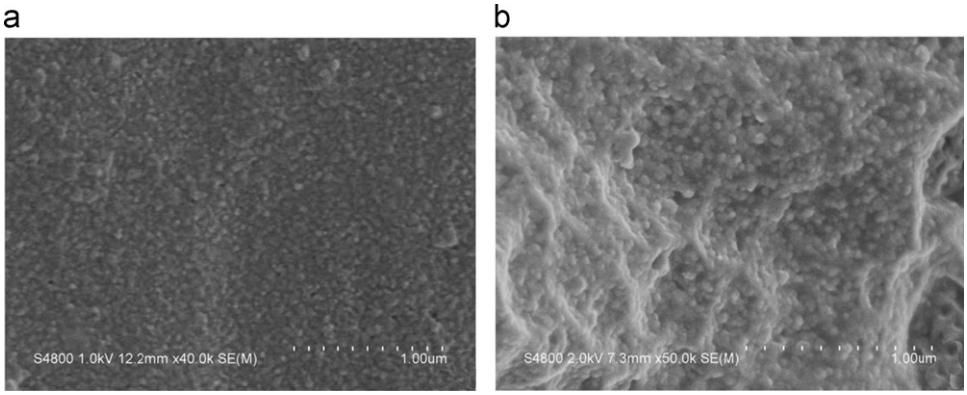

Fig. 2. The SEM micrograph of the surface of gold electrode after modified by antibody-functionalized magnetosomes (a) and normal antibody (b).

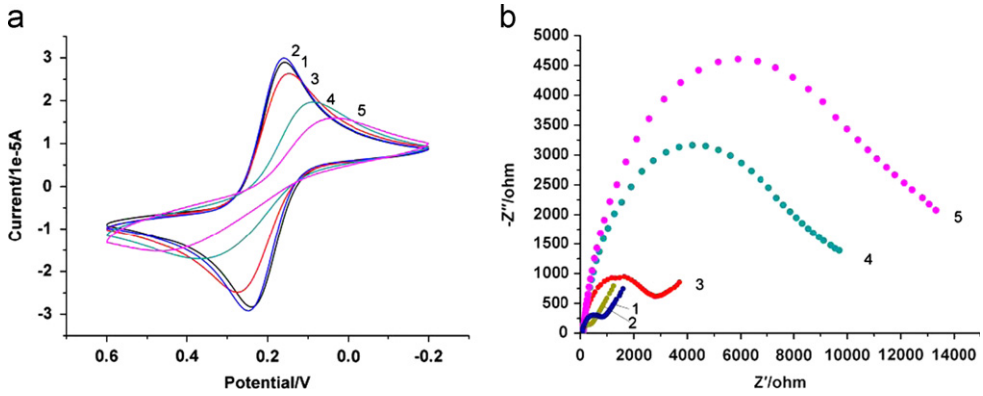

Fig. 3. CV (a) and EIS (b) of each step of the modified gold electrode: (1) bare gold electrode; (2) PANI/Au/bare gold electrode; (3) [D(n-C_4)Im][PF_6]/ PANI/Au/bare gold electrode; (4) SEB antibody-functionalized magnetosomes/[D(n-C_4)Im][PF_6]/PANI/Au/bare gold electrode; (5) BSA/SEB immuno-magnetosomes/[D(n-C_4)Im][PF_6]/ (PANI/Au)/bare gold electrode.

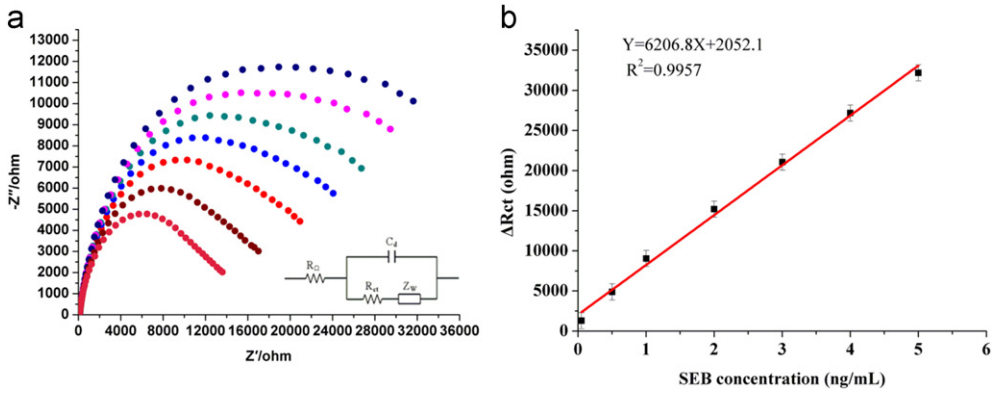

Fig. 4. The EIS (a) of the self-assembled immunsensor for detection of different concentration SEB, along the arrow the concentration was 5 ng/mL, 4 ng/mL, 3 ng/mL, 2 ng/mL, 1 ng/mL, 0.5 ng/mL and 0.05 ng/mL; Standard curve (b).

(40.76%) calculated from BCA experiment further indicated the successful coupling of the SEB antibodies to magnetosomes.

3.2. Characteristics of the modified gold electrodes

Fig. 2 showed SEM images of the surface of the gold electrodes after incubation with SEB antibody-functionalized magnetosomes (a) and normal SEB antibodies (b). A large amount of information can be concluded from the images through comparing Fig. 2a with b. Among them, the most outstanding characteristic is that Fig. 2a showed a smooth and dense film on the surface of the gold electrodes. This may be caused by several reasons, such as the better dispersity of the immuno-magnetosomes and the application of the layer-by-layer assemblies, which can precisely control the thickness of the films at a nanometer level. More importantly, the formation of the film provides a possibility to reduce the detection times.

Furthermore, both CV and EIS were investigated to check the electrochemical behavior of the as-prepared gold electrodes after each step of the electrochemical immunosensor construction. Fig. 3b shows the EIS curves of each step of the modified gold electrode. An increase in the impedance values was observed owing to blockage of the channel of electrons caused by the large increase in the relative thickness of the surface of the gold electrode, which indicated that the gold electrode had been modified successfully. And a well-defined redox peak and much faster transfer electrons of the as-fabricated sensor could be found in the CV curves (Fig. 3a), which is mainly attributed to the use of magnetosomes. Meanwhile, [D(n-C_4)Im][PF_6] and PANI/Au also played a crucial role in the above results. These results demonstrate that the proposed strategy can be successfully used for immunoassay, which further confirmed the success in the immunosensor design.

3.3. Performance of immuno-magnetosomes-based sensor

Under optimal conditions, the sensitivity of the electrochemical immunoassay based on magnetosomes was investigated by varying different concentrations of SEB. When the SEB antigen is bound with the anti-SEB antibody immobilized on the electrode, there would be an additional layer to block the electron diffusing from the solution to the surface of the electrode which resulted in an increased impedimetric response of our immunosensor. As shown in Fig. 4a, the impedimetric response of the immunosensor increased along with the increase of the concentration of SEB reacted with immobilized antibody on the electrode surface in PBS solution. The linear response range and detection limit of this immunosensor were calculated through standard curve (Fig. 4b) achieved from the detection of different concentrations (0.05 ng/mL, 0.5 ng/mL, 1 ng/mL, 2 ng/mL, 3 ng/mL, 4 ng/mL, and 5 ng/mL) of SEB standard solution at 37 °C for 20 min using the as-fabricated sensor. The values of impedance obtained from the circuit diagrams exhibited a good linear response in the range from 0.05 ng/mL to 5 ng/mL with a correlation coefficient (R^2) of 0.9957 and a detection limit of 0.017 ng/mL, which is lower than the sensor fabricated without magnetosomes (0.033 ng/mL, Fig. S3). The improved electron signal transportation not only

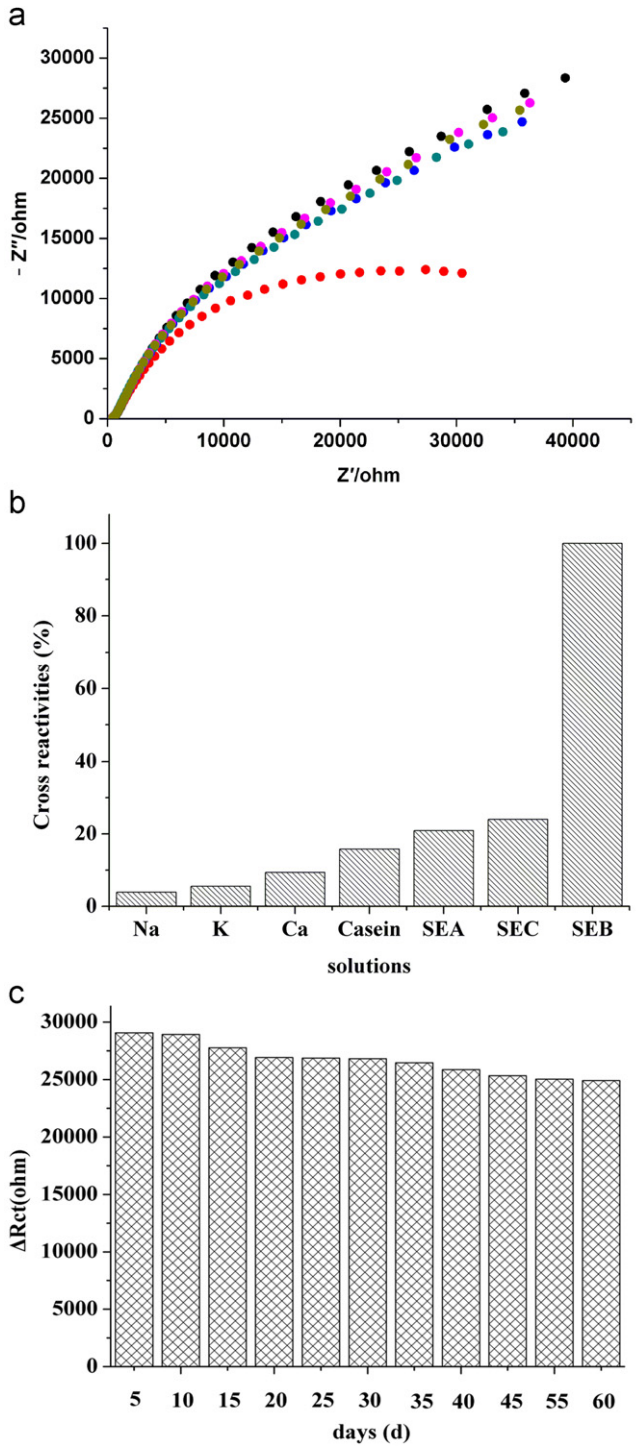

Fig. 5. The reproducibility (a), specificity (b) and stability (c) of the response signal.

attributed to the good dispersity of the antibody-functionalized magnetosomes but also PANI/Au and [D(n-C_4)Im][PF_6].

The specificity of this immunosensor to the same concentration (1×10^{-3} mol/L) of various SEs (SEA, SEB, and SEC), some protein (Casion) and some metal ions (Na^+, Ca^{2+}, K^+) that may be present in dairy products were evaluated by their EIS response change values (ΔRet) obtained from electrochemical detection. Cross reactivity (%) was as follows: cross reactivity = 100 × ΔRet of competitor/ΔRet of SEB. Fig. 5b showed that the adsorption ability

Table1
Recovery results of prepared immunosensor in low fat milk ($n=3$).

Samples	Added concentration (ng/ml)	ΔRet (Ω) (mean+SD)	Detected concentration (ng/ml) (mean+SD)	Recovery (%)
Defatted milk powder	0.5	4783 ± 1.7	0.44 ± 0.0003	88
	2	13,410 ± 2.6	1.83 ± 0.0004	92
	4	22,038 ± 1.3	3.22 ± 0.0002	81
Defatted milk	0.5	4659 ± 1.2	0.42 ± 0.0002	84
	2	15,893 ± 2.1	2.23 ± 0.0003	112
	4	29,176 ± 1.4	4.37 ± 0.0002	109
Fresh milk	0.5	5652 ± 2.3	0.58 ± 0.0004	116
	2	15,273 ± 1.3	2.13 ± 0.0002	107
	4	31,410 ± 1.7	4.73 ± 0.0003	118

Table 2
Immunosensor for the actual sample measurement.

Milk samples		Ret (Ω)	Enterotoxin detected (ng/mL)
Raw milk	1	7538	0.37
	2	7346	0.16
	3	8770	1.69
Sterilized milk	4	7092	—
	5	6987	—

Note: In samples 4 and 5, the Ret out of the linear response range of this immunosensor indicates no SEB in milk samples.

of SEB is significantly stronger than the others, which revealed a good specificity of this sensor.

After detection, the gold electrode was eluted with NaOH solution (1.2 mol/L) repeatedly to study the reproducibility of this immunosensor by EIS measurement. The results showed that the response signals were reduced by 0.31%, 0.92%, 1.7%, and 4.1% (Fig. 5a) compared with the original values, that is to say a good response signal could be obtained after repeating four times. On further elution with NaOH solution, the response signal showed a large change, therefore this immunosensor could be regenerated for four times.

Then the developed electrochemical immunosensor was scanned in $K_3[Fe(CN)_6]/K_4[Fe(CN)_6]$ solution (2.5 mmol/L) by performing CV measurements for 100 cycles. The result indicated that a good repeatability of this sensor was acquired, meanwhile a relative standard deviation of 5.02% for SEB detection was obtained (1 ng/mL, $n=9$).

Furthermore, the long-time stability of the as-prepared sensor was also investigated during a 60 day period at 4 °C. The results (Fig. 5c) showed that there was no significant change in the impedance response, where the values of impedance decreased to 0.45%, 4.5%, 7.8%, 11.0%, 13.8% and 14.3% after 10 days, 20 days, 30 days, 40 days, 50 days and 60 days, respectively, indicating that this sensor has good stability. All these good performances of the developed sensor may be due to the use of magnetosomes, which can offer good biocompatibility to maintain the activity of the SEB antibodies for prolonged time. Accordingly, it is possible to detect SEB in the field of monitoring using this sensor.

3.4. Detection of SEB in milk samples

The recoveries were calculated according to the measurement (Table 1), and the recoveries range from 81% to 118% (Table 1), showing a good performance of the sensor and potential in SEB detection in milk. Meanwhile, from the results of actual sample measurements, we can see that SEB was detected in raw milk at

concentrations of 0.37 ng/mL, 0.16 ng/mL and 1.69 ng/mL, and SEB was not detected in sterilized milk (Table 2).

4. Conclusion

This present work described a simple, rapid and sensitive approach for the fabrication of an electrochemical immunosensor based on a gold electrode modified with a composite film of SEB immuno-magnetosomes/[D(n-C_4)Im][PF_6]/(PANI/Au). First, the magnetosomes used not only offered a larger specific surface area to increase the immobilization amount of antibodies and immunoreaction rate, but also provided a good dispersity to form a smooth and dense film on the gold electrode. Second, the PANI/Au that was applied to the gold electrode could enhance the response signals of the immunosensor to SEB. Finally, [D(n-C_4)Im][PF_6] was provided as an electrolyte to provide good conductivity and a stable electrochemical response. Under optimal conditions, the developed immunosensor showed a good linear response in the range from 0.05 to 5 ng/ml (R^2=0.9957) with a detection limit as low as 0.017 ng/ml, compared with the one without magnetosomes (0.05–5 ng/mL, 0.033 ng/mL), this developed immunosensor showed a wider response range and a reduced detection limit. And a good specificity with little adsorption to SEA, SEC and Na^+, K^+, Ca^{2+} was obtained. Moreover, the immunosensor exhibited a good long-time stability at 4 °C reaching up to 60 days, which showed a relatively long working life. Meanwhile the immunosensor could be regenerated four times using NaOH elution. The sensor also displayed a good repeatability with a relative standard deviation of 5.02% for SEB detection (1 ng/mL, n=9). Meanwhile, high recoveries in the range of 81%–118% were achieved and successfully applied to raw milk and sterilized milk. All of the above fully demonstrated that this fabrication method has a wide linear range, a low detection limit, a good recovery and a high reproducibility, and the most important is the possibility to use them in situ. Therefore, the electrochemical immunosensor developed is a promising tool for routine monitoring to detect SEB in food.

Acknowledgments

This work has been supported by the "973" National Basic Research Program of China (No. 2012CB720804), National Research Program (No. 2011BAK10B03), and the Commonweal project of the Ministry of Agriculture (Nos. 201003008-08, No. 201203069–1).

Appendix A. Supporting information

Supplementary data associated with this article can be found in the online version at http://dx.doi.org/10.1016/j.talanta.2012.12.053.

References

[1] W.-C. Tsai, P.-J. Pai, Microchim. Acta. 166 (2009) 115–122.
[2] N. Balaban, A. Rasooly, Int. J. Food Microbiol. 61 (2000) 1–10.
[3] G. Blaiotta, D. Ercolini, C. Pennacchia, V. Fusco, A. Casaburi, O. Pepe, F. Villani, J. Appl. Microbiol. 97 (2004) 719–730.
[4] L. Macaluso, C. Lapeyre, S. Dragacci, Analusis 26 (1998) 300–303.
[5] B. Liang, Y. Zhang, A. Liu, Y. Zhou, F. Chen, X. Wang, Appl. Biochem. Biotechnol. 164 (2011) 831–840.
[6] P. Xue, Y. Li, Z. Zhang, A. Fu, F. Liu, X. Zhang, Y. Sun, L. Chen, B. Jin, K. Yang, Microchim. Acta 174 (2011) 167–174.
[7] R. Jung, G. Terplan, Food Agric. Immunol. 5 (1993) 107–114.
[8] M. Yang, S. Sun, Y. Kostov, A. Rasooly, Anal. Biochem. 416 (2011) 74–81.
[9] C.E. Kientz, A.G. Hulst, E.R.J. Wils, J. Chromatogr. A 757 (1997) 51–64.
[10] M. Klotz, S. Opper, K. Heeg, S. Zimmermann, J. Clin. Microbiol. 41 (2003) 4683–4687.
[11] M. Principato, J.M. Njoroge, A. Perlloni, M.O. Donnell, T. Boyle, J.R.L. Jones, J. Food Sci. 75 (2010) T141–T147.
[12] Z.-G. Chen, D.-Y. Tang, Bioprocess Biosyst. Eng. 30 (2007) 243–249.
[13] M.P. Chatrathi, J. Wang, G.E. Collins, Biosens. Bioelectron. 22 (2007) 2932–2938.
[14] M.M. Ngundi, G.P. Anderson, Biosens. Bioelectron. 22 (2007) 3243–3246.
[15] P.T. Charles, F. Velez, C.M. Soto, E.R. Goldman, B.D. Martin, R.I. Ray, C.R. Taitt, Anal. Chim. Acta 578 (2006) 2–10.
[16] C. Ruan, K. Zeng, O.K. Varghese, C.A. Grimes, Biosens. Bioelectron. 20 (2004) 585–591.
[17] H.-C. Lin, W.-C. Tsai, Biosens. Bioelectron. 18 (2003) 1479–1483.
[18] K.D. King, G.P. Anderson, K.E. Bullock, M.J. Regina, E.W. Saaski, F.S. Ligler, Biosens. Bioelectron. 14 (1999) 163–170.
[19] F. Li, L. Mei, Y. Li, K. Zhao, H. Chen, P. Wu, Y. Hu, S. Cao, Biosens. Bioelectron. 26 (2011) 4253–4256.
[20] J.-D. Qiu, H.-Z. Peng, R.-P. Liang, J. Li, X.-H. Xia, Langmuir 23 (2007) 2133–2137.
[21] M. Labib, M. Hedström, M. Amin, B. Mattiasson, Anal. Bioanal. Chem. 393 (2009) 1539–1544.
[22] Z.-G. Chen, Bioprocess Biosyst. Eng. 31 (2008) 345–350.
[23] T. Selvaraju, J. Das, S.W. Han, H. Yang, Biosens. Bioelectron. 23 (2008) 932–938.
[24] C.A. Betty, Biosens. Bioelectron. 25 (2009) 338–343.
[25] M.M. Yallapu, S.F. Othman, E.T. Curtis, B.K. Gupta, M. Jaggi, S.C. Chauhan, Biomaterials 32 (2011) 1890–1905.
[26] S.A. Ansari, Q. Husain, Biotechnol .Adv. 30 (2012) 512–523.
[27] F. Li, R. Zhou, K. Zhao, H. Chen, Y. Hu, Talanta 87 (2011) 302–306.
[28] S. Laurent, S. Dutz, U.O. Häfeli, M. Mahmoudi, Adv. Colloid Interface Sci. 166 (2011) 8–23.
[29] H. Liu, S. Li, L. Liu, L. Tian, N. He, Biosens. Bioelectron. 26 (2010) 1442–1448.
[30] A.J. Cole, A.E. David, J. Wang, C.J. Galbán, H.L. Hill, V.C. Yang, Biomaterials 32 (2011) 2183–2193.
[31] E. Arzum, P.M. Isabel, L. Anabel, B. Alessandra, D.V. Manel, A. Salvador, Sens. Actuators B Chem. 114 (2006) 591–598.
[32] E. Paleček, M. Fojta, Talanta 74 (2007) 276–290.
[33] S. Campuzano, B.E.-F. de Ávila, J. Yuste, M. Pedrero, J.L. García, P. García, E. García, J.M. Pingarrón, Biosens. Bioelectron. (2010) 1225–1230.
[34] M. Racuciu, D.E. Creanga, A. Airinei, V. Bidescu, J. Optoelectron. Adv. Mater. 10 (2008) 2928–2931.
[35] M.J. Bonder, Y. Zhang, K.L. Kiick, V. Papaefthymiou, G.C. Hadjipanayis, J. Magn. Magn. Mater. 311 (2007) 658–664.
[36] M. Büttner, P. Weber, C. Lang, M. Röder, D. Schüler, P. Görnert, P. Seidel, J. Magn. Magn. Mater. 323 (2011) 1179–1184.
[37] T.-X. Fan, S.-K. Chow, D. Zhang, Prog. Mater. Sci. 54 (2009) 542–659.
[38] M. Maas, P. Degen, H. Rehage, H. Nebel, M. Epple, Colloids Surf. A:Physicochem. and Eng. Aspects 354 (2010) 149–155.
[39] T. Hennebel, B. De Gusseme, N. Boon, W. Verstraete, Trends Biotechnol. 27 (2009) 90–98.
[40] E. Alphandéry, L. Lijeour, Y. Lalatonne, L. Motte, Sens. Actuators B 147 (2010) 786–790.
[41] L. Zhang, H. Peng, P.A. Kilmartin, C. Soeller, R. Tilley, J. Travas-Sejdic, Macromol. Rapid Commun. 29 (2008) 598–603.
[42] X. Yang, Q. Xie, S. Yao, Synth. Met. 143 (2004) 119–128.
[43] T.-Y. Wu, S.-G. Su, H.P. Wang, I.W. Sun, Electrochem. Commun. 13 (2011) 237–241.
[44] Y. Chen, Y. Zhang, F. Ke, J. Zhou, H. Wang, D. Liang, Polymer 52 (2011) 481–488.
[45] R. Donato, M. Migliorini, M. Benvegnú, J. Dupont, R. Gonçalves, H. Schrekker, J. Solid State Electrochem. 11 (2007) 1481–1487.
[46] W. Zhao, J.-J. Xu, H.-Y. Chen, Electroanalysis 18 (2006) 1737–1748.
[47] T. Matsunaga, T. Sakaguchi, F. Tadakoro, Appl. Microbiol. Biotechnol. 35 (1991) 651–655.
[48] C.-D. Yang, H. Takeyama, T. Tanaka, T. Matsunaga, Enzyme Microb. Technol. 29 (2001) 13–19.
[49] K. Zhu, H. Pan, J. Li, K. Yu-Zhang, S.-D. Zhang, W.-Y. Zhang, K. Zhou, H. Yue, Y. Pan, T. Xiao, L.-F. Wu, Res. Microbiol. 161 (2010) 276–283.
[50] J. Gruber, G.G. Wright, J. Bacteriol. 99 (1969) 18–24.
[51] J.M. Yarwood, J.K. McCormick, M.L. Paustian, V. Kapur, P.M. Schlievert, J. Bacteriol. 184 (2002) 1095–1101.
[52] X. Wang, Y. Shen, A. Xie, S. Li, Y. Cai, Y. Wang, H. Shu, Biosens. Bioelectron. 26 (2011) 3063–3067.
[53] X. Zhang, J. Zhu, N. Haldolaarachchige, J. Ryu, D.P. Young, S. Wei, Z. Guo, Polymer 53 (2012) 2109–2120.
[54] H. Shan, Y. Lu, Z. Li, M. Li, Y. Cai, X. Sun, Y. Zhang, Chin. J. Catal. 31 (2010) 289–294.